Optics Communications 285 (2012) 3373–3377

Contents lists available at SciVerse ScienceDirect

Optics Communications

journal homepage: www.elsevier.com/locate/optcom

Designs of apertureless probe with nano-slits for near-field light localization and concentration

Youngkyu Lee [a,*], Xiaojing Zhang [b,*]

[a] Department of Electrical Engineering, the University of Texas at Austin, Austin, TX 78712 USA
[b] Department of Biomedical Engineering, the University of Texas at Austin, Austin, TX 78712 USA

ARTICLE INFO

Article history:
Received 23 December 2011
Received in revised form 15 March 2012
Accepted 18 March 2012
Available online 3 April 2012

Keywords:
Near field
Plasmons
Coupler

ABSTRACT

This paper presents recent studies on nano-patterned plasmonic probes that can provide highly localized and enhanced light for the near-field scanning optical microscopy. The mechanism to realize such localized light source is introduced and numerically characterized in the near field. In addition, the attainable wideband operation of the plasmonic probe through the proper design is also discussed with particular attention to developing potential applications in the near-field scanning optical microscopy.

Published by Elsevier B.V.

1. Introduction

Near-field scanning microscopy (NSOM) is a versatile tool for investigating the sample surfaces, allowing the imaging of both optical signature and topographic information. By probing near-field interactions within the localized region of sample, high resolution optical images, which cannot be reached through the conventional optics, has been achieved with various probe designs. In particular, aperture-based NSOM probe [1,2] in the transmission mode has shown promising results in terms of high-resolution imaging while guiding and focusing electromagnetic (EM) energy over the damping mode of waveguide of the small aperture. To obtain quality optical images in near-field, fundamental, physical requirements have to be satiated. First, the waveguide geometry of a probe including the aperture geometry needs to support the efficient transmission of optical energy; and second, a sharp tip dimension allowing access to the small region of interest is also necessary. By observing the near-field interaction which is coupled through the small aperture, one would achieve the high resolution of optical images better than 50 nm [1,2]. For the past decades, various aperture-based NSOM probe designs have been reported to satisfy such qualifications and break the diffraction limit of conventional optics, taking advantage of the local near field [3–5]; however, the inherent low optical transmittance of NSOM probes associated with the small dimension of aperture for the high-resolution imaging in general limits the performance of near-field scanning by impeding the signal discrimination over strong background noise signals.

To overcome such low optical transmission of aperture-based probe designs, the recent progress in NSOM probe design has been made utilizing the property of surface plasmon wave [6,7], which is following the evanescent mode of propagation at the metal and dielectric interface. In plasmonic nano-photonics, effective focusing and enhancing of near-field light within the small region of interest may rely on the configuration of metal geometry used [8–13]: the improved throughput with effective light confinement has been achieved by using the geometries for diffractive light focusing [8], build-up of aperture resonance [9,10], nano-antenna at aperture [11], and geometrical plasmon focusing [12,13]. Among the prominent progresses, one important probe design was devised [14] through the use of periodic corrugations perforated in metal film. One can further utilize the optical energy, coupled through an aperture, in a more efficient way by focusing plasmonic surface waves before being dissipated by the propagation loss. A metallic probe with a tip aperture and concentric corrugations on its face could feature large field enhancement in the near field of the tip apex [14]. Following the demonstration of such diffractive SPP focusing for NSOM applications, similar probe configurations have been studied in order to provide the enhanced signal to noise ratio (S/N) [15,16]. Although late studies on localized near-field enhancement of aperture-based probe design claim that the use of surface wave is being effective for the near-field focusing and enhancement, overall optical energy available for near-field scanning is sorely dependent on the limited optical energy coupled through the waveguide geometry of probe and small aperture. This allows the use of only fraction of impinging energy; thus, one may envision the probe designs that can utilize the impinging light in a more efficient way without suffering from the cut-off mode of the waveguide and low transmittance of small aperture.

In this paper, we present our recent theoretical study on novel plasmonic probe designs, providing the mechanism of efficient near-field

* Corresponding authors.
E-mail addresses: youngkyu.lee@mail.utexas.edu (Y. Lee), John.Zhang@engr.utexas.edu (X. Zhang).

0030-4018/$ – see front matter. Published by Elsevier B.V.
doi:10.1016/j.optcom.2012.03.016

focusing and localization [17]; and further extended the study on plasmonic probe featuring wideband operation is also presented. The proposed probe configuration involves the designed non-local Surface Plasmon Plariton (SPP) coupler (see Fig. 1) launching surface plasmon waves in a unidirectional way, and metal-coated probe body featuring a sharp dimension of apertureless tip. Slit-based non-local coupler designs [19,20] are employed to efficiently translate the impinging light into the SPPs on prove faces, and metal-coated sharp pyramidal geometry is considered to geometrically guide the surface energy at small tip apex. Unlike the conventional aperture-based probe designs in which the aperture is located at the cut-off region of probe waveguide, the proposed probe configurations may utilize more optical energy before being dissipated by the modal rejection. Herein, the metal-coated pyramidal probes are presented with various SPP generation mechanisms, showing extremely large field enhancement and high optical resolution. The proposed probes are characterized in the near field with the finite-integration-technique (FIT) based software package, CST Microwave Studio. In addition to the numerical study on the near-field focusing and enhancement for NSOM applications, we discuss potential ways to introduce the wide bandwidth of operation to the probe geometry with a non-local SPP coupler. By employing a proper design of the SPP coupler, a plasmonic probe possibly provides the desired spectral response of operation.

2. Apertureless plasmonic probe designs

2.1. Single slit-based SPP couplers for the near-field focusing and localizing

We consider metal-coated, pyramidal-shaped dielectric probe geometry for the light localization and concentration, which can realized within the current silicon-based MEMS technologies [18] and nano-fabrication technique such as the bulk micromachining and focused ion beam (FIB) etching. The proposed probe configuration consists of sharp metallic (silver) apertureless tip with a diameter of 100 nm and a slit-based non-local SPP coupler perforated in 250 nm thick Ag film on probe face. Unlike the classical aperture-based probe (with local light source) in which the most incident light is being cut-off before reaching to the tip aperture, a probe with non-local SPP couplers can utilize the impinging optical energy in a more efficient way without suffering cut-off of waveguide mode. Upon the utilization of non-local coupler, launched SPPs can be guided toward the tip side and focused by sharp probe geometry, enabling highly localized near-field enhancement at tip apex. To translate incident light to SPP in a more efficient way, two different SPP generation mechanisms [19,20] are employed and integrated with probe geometry. Single slit supporting non-fundamental mode of waveguiding inside is mounted to realize type A probe, unidirectionally generating SPPs with an oblique incident of light. Optimal design parameter, slit width of 371 nm [17], is chosen to realize highly directive SPP generation at 633 nm with a given tilted illumination (tilting angle of 54.4°). In type B probe, a single slit (100 nm in width) operating with only fundamental mode is mounted and backed Bragg reflector to direct coupled SPPs in unidirectional manner. Similar to type A probe design, generated SPPs can be guided along the face to tip apex with a sharp probe tip geometry. For both type A and type B probe, non-local couplers were placed 1000 nm distant from a tip apex along the probe face.

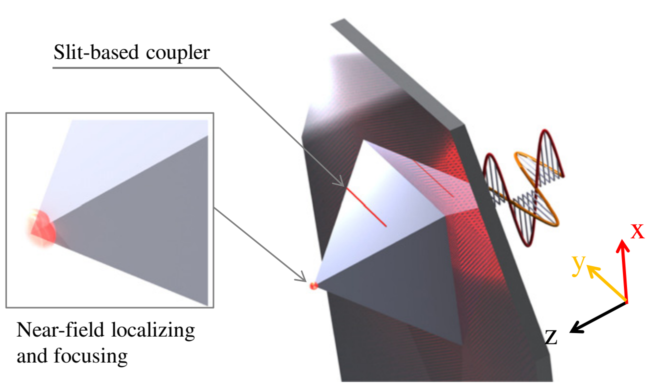

Fig. 1. Probe geometry of interest, consisting of metallic probe tip and slit-based SPP coupler.

With a classical single aperture probe, both type A and type B probe are numerically characterized and compared in near field of the tip. Radially polarized illumination operating at 633 nm is considered to maximally take advantage of four SPP couplers on probe faces and to provide the constructive interference of axially polarized electric field E_z. The calculated electric field intensity and the electric energy density of each probe are presented in Fig. 2. To evaluate the optical resolution of proposed probes, the full-width-at-half-maximum (FWHM) is defined by the distribution of the electric energy density near the probe tip. Both calculated field distribution and electric energy density are compared to that of a canonical single aperture probe at 20 nm distance from the tip. Compared to the conventional single aperture probe, design A and design B probes features extremely large near-field enhancements by a factor of 2119 and 1023, respectively. Similarly, electrical energy density of type A is boosted more than 4×10^6 times, and which of type B is improved by 6 orders without compromising FWHM. The calculated FWHMs of the three probes are: 148.84 nm (canonical aperture probe), 138.02 nm (Type A) and 171.3 nm (Type B). Within 100 nm range of tip-sample distance, the calculated FWHMs of type A and B probes are contained under 200 nm, and both probes still hold huge energy density enhancement as shown in Fig. 3.

One important feature of proposed probe geometries is that the near-field optical resolution (FWHM) attainable in near field is primarily determined by the physical dimension of the tip apex as reported in a previous study [21]. By reducing the tip size, one may obtain better optical resolution and improved near-field enhancement. Fig. 4 shows the effect of tip size on the near-field enhancement and confinement especially for the type A probe. Type A with various tip diameters is characterized in near field by the electric energy profiles, specifically FWHM at 20 nm tip-sample distance along the x-direction, are calculated.

As presented the maximum value of near-field intensity is inversely proportional to the tip dimension while the defined optical resolution (i.e. FWHM) is in the opposite proportionality. We note that such relationship between the tip size and near-field intensity is clearly distinctive from that of aperture-based probe, which is relying on the evanescent mode of transmission through small aperture showing extremely low transmission efficiency as the aperture size reduces. In this regard, the development of efficient NSOM probe may take advantage of our approach and become subject to realizing the sharp probe tip geometry with a proper design of efficient non-local SPP coupler.

2.2. Array of slits on apertureless probe for wideband operation

As discussed in the previous section, we have recognized that the near-field focusing and enhancement at probe tip can be achieved by efficient SPPs generation and proper design of near-field guiding geometry. This concept may be expanded to introduce the specific spectral functions for some applications. Since the spatial resolution of the proposed probe configuration counts on the geometrical sharpness of tip apex as shown in our previous study [17] and elsewhere [21], the proposed apertureless NSOM probe may feature various operating spectrum following that of the non-local coupler designed for specific purpose of interest. Among the desired spectral responses that can be achieved through the well-known coupler designs [22] at the radio frequency (RF), one may envision the wide bandwidth of operation for harvesting the various spectral signatures of specimen with a

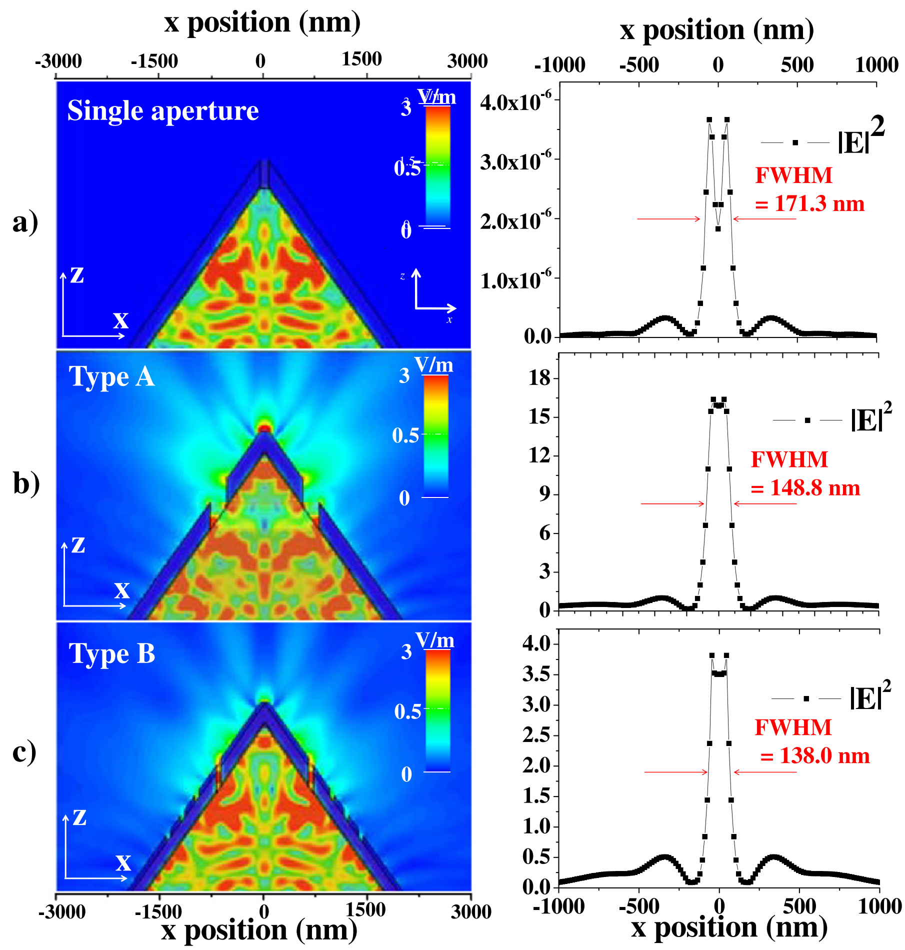

Fig. 2. Calculated |E| field distributions of 3 different probes in x–z plane (left column) and $|E|^2$ distribution along x axis with tip-sample distance of 20 nm (right column): (a) a classic single aperture probe with 100 nm-sized rectangular aperture, (b) type A probe, and (c) type B probe.

single probe. Since previously reported probe designs utilizing the diffractive focusing and near-field enhancement [14–16] are of the design for specific wavelength of operation, it would be impractical to observe wideband optical signatures with identical optical resolution. In contrast, the apertureless probe with wideband SPP coupler is being robust to the wavelength of operation (see Fig. 3), and may allow us to study the light-matter interaction at various wavelengths without degrading optical resolution. Studying the absorption spectra of specimen in near field, for instance, may broaden the scope of near-field optical microscopy by adopting the multi-color imaging of sample. In optic regime, the light–matter interaction varies with the change of operating frequency, so that one may achieve the hyper-spectral images of sample without having the target specimens stained with dyes.

To realize wideband operation, we may employ and modify a slit-based coupler design methodology which is frequently referred in the

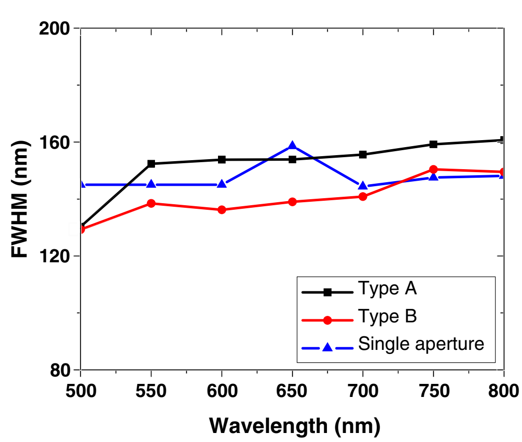

Fig. 3. Spectral characteristic of three probes: type A, type B, and classical single aperture probe. FWHM along x axis is calculated at tip-sample distance of 20 nm.

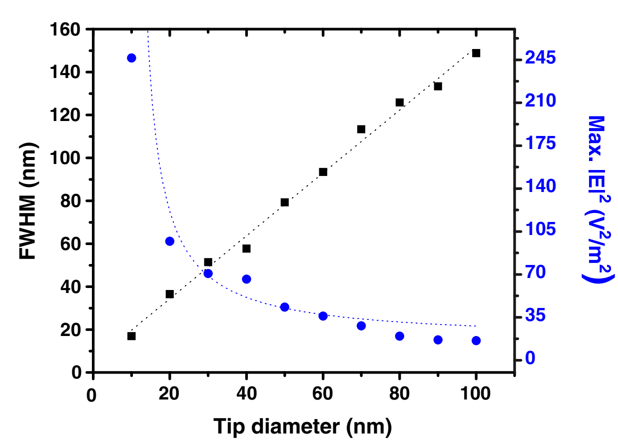

Fig. 4. Computed near-field characteristics of type A probe with various tip diameter: optical resolutions (FWHMs) are calculated at tip-sample distance of 20 nm along x-direction (black squares) and the highest intensity of electric energy is calculated (blue circles). Note that dotted lines are fitting curves.

microwave engineering applications [22]. By manipulating the phase and intensity of wave out-coupled from each slit, one can tailor the overall spectral response of coupler. The proposed SPP coupler consists of an array of subwavelength-sized slits, each of which supports only the fundamental mode of waveguide inside; the array is designed following the rearranged series of Chebyshev polynomials to take advantage of fabrication convenience and to serve the wide bandwidth of operation. The transfer function S arranged from Chebyshev polynomials ($T_n(\sec\zeta\cdot\cos\psi)$) of the first kind for an array of N slits is derived and given as

$$S = \begin{cases} \sum_{i=0}^{(N-1)/2} T_{2i}(\sec\zeta\cos\psi) & \text{for } N = \text{odd number} \\ \sum_{i=1}^{N/2} T_{2i-1}(\sec\zeta\cos\psi) & \text{for } N = \text{even number} \end{cases},$$

where ζ *is the* edge of pass band over and phase span of ψ.

We note that the presented coupler design is being based on the summation of the Chebyshev responses of equal amplitude. Unlike the general, single Chebysheve response, the expected overall response S would not be equal-ripple spectra. Under a given geometry inside probe where the incident waves obliquely impinge on the slit array, the operating bandwidth can be controlled by the separation distance between each slit. We integrate the slit-based wideband SPP coupler to probe geometry and observe the near-field characteristics of probe.

To put the future experimental demonstration towards being more practical in terms of a simple optical setup configuration, it may be beneficiary to demonstrate the performance probe operating under the illumination of linearly polarized lights. In contrast to the case in which the radially polarized light is being used, the alignment of optics may not be required, and the coherent plane wave may be used to excite the probe. To theoretically demonstrate, the probe having a coupler on its single face is designed, and characterized in near field under the illumination of linearly polarized plane light operating at 633 nm. In this probe configuration, the coupler integrated on the face of probe launches SPPs in unidirectional way over the wide bandwidth of operation, and the sharp probe geometry guides SPPs focus at tip apex (radius of 40 nm). The calculated electric field intensity and electric energy density of the probe with wideband SPP coupler in near field are presented in Fig. 5(b), comparing with the probe where a single slit coupler is used (Fig. 5(a)). The wideband SPP coupler consists of 5 identical slits with the width of 50 nm and separation of 100 nm, and the first slit of the array is located 1500 nm away from the tip apex. In the case in which the single-slit coupler is being used, the SPPs are launched in bi-directional manner due to the existing fundamental mode supported only by such small slit. The passband spectra of the probe with wideband coupler are compared with that with a single slit coupler and presented in Fig. 6.

The numerical study in Fig. 5 shows that the probe integrated with a 5-slit coupler (Fig. 5(b)) can guide and focus the near-field light within the very limited volume of interest (tip apex) in a more efficient way. In comparison to the performance of probe with single-slit coupler, that with 5-slit coupler features higher near-field enhancement (7 times higher in terms of near-field intensity) by the efficient generation of SPPs and geometrical nano-focusing while containing the optical resolution (i.e. FWHM) of around 70 nm. We note that the calculated values of optical resolution of both probes are identical, and it proves that the geometry-dependent optical resolution is still held for the case that the linearly polarized light is used similar to the early statement in the previous section.

The spectral response of proposed probe geometry in near field is characterized as well by observing the maximum value of electric energy density at the tip-sample distance of 20 nm (see Fig. 6). Two different probes have been numerically investigated and compared to each other: apertureless probe with a wide-band SPP coupler, and that with a single slit coupler. The numerical study in Fig. 6 shows that the near-field enhancement can be achieved within the wide bandwidth of operation by adopting the slit array. In comparison to the probe with single-slit coupler, the probe with 5-slit array shows 11.05 dB higher electric energy density on average (with 1.23 dB less standard deviation) over the spectrum ranging from 500 nm to 810 nm.

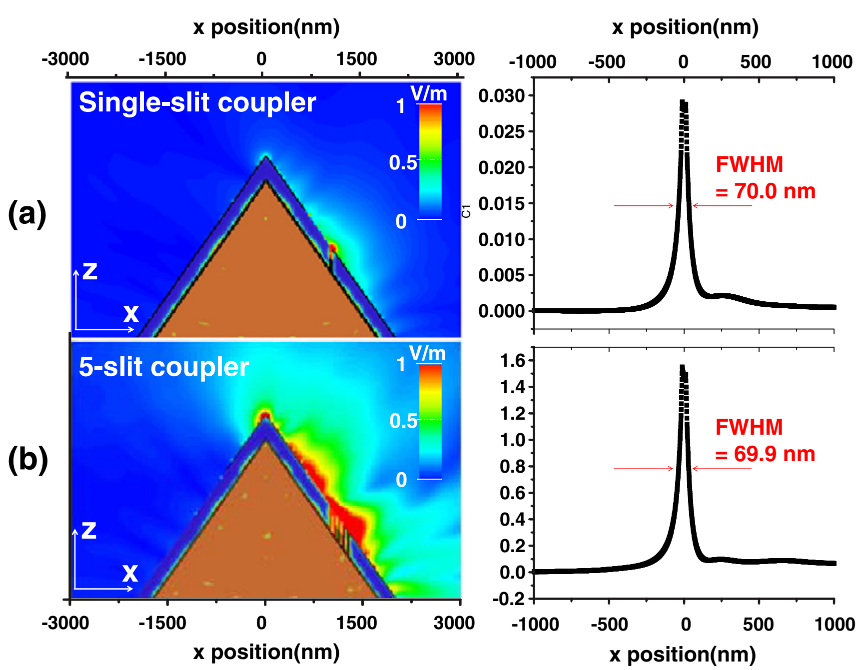

Fig. 5. Calculated |E| field distributions of 2 different probes in x–z plane (left column) and $|E|^2$ distribution along x axis with tip-sample distance of 20 nm (right column): (a) apertureless probe with 5-slit array, and (b) single slit coupler.

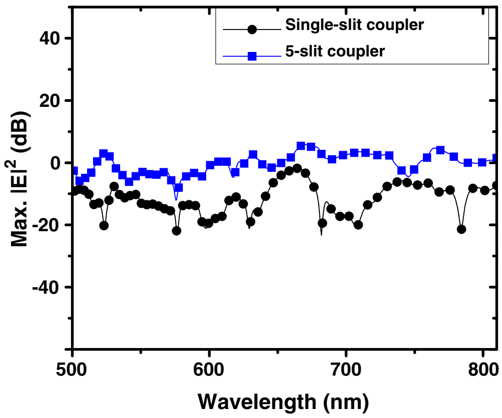

Fig.6. Maximum values of $|E|^2$ of two probes calculated over the spectral range of interest. $|E|^2$ is calculated at tip-sample distance of 20 nm and scaled in decibel. Note that the calculated spectrum is normalized to the intensity of impinging light (0 dB).

3. Discussion and conclusion

The property of surface plasmons at the metal and dielectric interface offers an intriguing way to focusing and localizing light within sub-wavelength scale volume. Herein, we summarize the key findings from an intensive numerical study on the designs of plasmonic scanning probe. Proposed designs can provide extremely large near-field enhancement while containing electromagnetic energy in small volume, while offering the geometry-dependent spatial resolution. It is also discussed that desired spectral function, specifically wideband operation, maybe introduced to the NSOM probe by choosing a proper design methodology of non-local SPP coupler. Throughout manipulating the configuration of slit-based SPP coupler, a scanning probe appealing for wideband operation may be obtained. We believe that our probe designs can be realized within the scope of standard micro-/nano-fabrication technologies that reported elsewhere [17], while opening a new generation of the near-field scanning optical microscopy that serves the high optical-resolution imaging within tunable spectrum.

Acknowledgements

This research was performed at the Biomedical Engineering, Microelectronics Research Center (MRC) at UT Austin. We gratefully acknowledge the financial support from the National Science Foundation (NSF CAREER Award Grant No. 0846313) and DARPA Young Faculty Award (N66001-10-1-4049).

References

[1] D.W. Pohl, W. Denk, M. Lanz, Applied Physics Letters 44 (1984) 651.
[2] U. Dürig, D.W. Pohl, F. Rohner, Journal of Applied Physics Letters 59 (1986) 3318.
[3] A. Harootunian, E. Betzig, M. Isaacson, A. Lewis, Applied Physics Letters 49 (1986) 674.
[4] E. Betzig, M. Isaacson, A. Lewis, Applied Physics Letters 51 (1987) 2088.
[5] E. Betzig, J.K. Trautman, Science 257 (1992) 189.
[6] H. Raether, Surface Plasmons on Smooth and Rough Surfaces and on Gratings, Springer-Verlag, 1988.
[7] J.A. Schuller, E.S. Barnard, W. Cai, Y.C. Jun, J.S. White, M.L. Brongersma, Nature Materials 9 (2010) 193.
[8] H.J. Lezec, A. Degiron, E. Devaux, R.A. Linke, L. Martin-Moreno, F.J. Garcia-Vidal, T.W. Ebbesen, Science 297 (2002) 820.
[9] X. Shi, L. Hesselink, Japanese Journal of Applied Physics 41 (2002) 1632.
[10] N.M. DuBay, L. Wang, E.C. Kinzel, S.M.V. Uppuluri, X. Xu, Optics Express 16 (2008) 2584.
[11] T.H. Taminiau, R.J. Moerland, F.B. Segerink, L. Kuipers, N.F. Van Hulst, Nano Letters 7 (2007) 28.
[12] C. Ropers, C.C. Neacsu, T. Elsaesser, M. Albrecht, M.B. Raschke, C. Lienau, Nano Letters 7 (2009) 2784.
[13] C.C. Neacsu, S. Berweger, R.L. Olmon, L.V. Saraf, C. Ropers, M.B. Raschke, Nano Letters 10 (2010) 592.
[14] Y. Wang, W. Srituravanich, C. S., X. Zhang, Nano Letters 8 (2008) 3041.
[15] Y. Wang, Y. Huang, X.J. Zhang, Optics Express 18 (2010) 14004.
[16] D.W. Kim, Y.C. Kim, O. Suwal, V. Jha, M.J. Park, S.S. Choi, Materials Science and Engineering B 149 (2008) 242.
[17] Y. Lee, A. Alu, X.J. Zhang, Optics Express 19 (2011) 25990.
[18] G.M. Kim, B.J. Kim, E.S. Ten Have, F. Segerink, N.F. Van Hulst, J. Brugger, Journal Of Microscopy 209 (2003) 267.
[19] F. López-Tejeira, Sergio G. Rodrigo1, L. Martín-Moreno, F.J. García-Vidal, E. Devaux, T.W. Ebbesen, J.R. Krenn, I.P. Radko, S.I. Bozhevolnyi, M.U. González, J.C. Weeber, A. Dereux, Nature Physics 3 (2007) 324.
[20] H. Kim, B. Lee, Plasmonics 4 (2009) 153.
[21] M. Stockman, Physical Review Letters 93 (2004) 137404.
[22] D.M. Pozar, Microwave Engineering, Addison Wesley, 1990.